Earth Gravity Assisted Inclination Change to Reduce Lunar Constellation Deployment ΔV

Darin C. Koblick and Joseph S. Choi
Raytheon Intelligence and Space, El Segundo, CA 90245

ABSTRACT

Dozens of international teams are sending orbiters, small satellites, rovers, and crewed missions to the Moon as we envision a permanent presence. These missions will require dedicated support infrastructure such as lunar communications and navigation services such as NASA's LunaNet and ESA's Moonlight initiatives. Lunar satellite constellations operate at different orbital inclinations for enhanced surface coverage, long term orbital stability, and geometric diversity. In this research, a numerical optimization technique is developed to change the inclination of an orbit by exploiting Earth's gravitational force under the full three-body Equations of motion. These inclination change maneuvers, bounded analytically by the Jacobi Constant, allow for the full 180° inclination changes. We found that these Earth gravity assisted inclination changes require less ΔV when change angles were greater than 45° vs single-impulse instantaneous maneuvers. For circular lunar orbit altitudes greater than 100 km, the total ΔV required for an Earth gravity assisted inclination change is less than 1.4 km/s (regardless of the angle) with transfer times less than ten days. Earth gravity assists enable a spacecraft to reduce its ΔV deployment costs up to 60% allowing for larger payload SWaP and enhanced mission capabilities.

1. INTRODUCTION

Low altitude lunar orbits may be unstable as large gravitational perturbations caused by mascons tug them down crashing the space vehicle into the surface [1]. It would be logical to select lunar orbits with higher altitudes, but many above 1,200 km altitude are also unstable (Lidov–Kozai effect [2]) from the large gravitational pull of the Earth. Earth's gravitational influence from a higher altitude lunar orbit can plummet a satellite into the surface by tugging down it's perilune or it can pull it's apolune up causing an escape from the Moon's gravitational influence [3]. This phenomenon has been observed on other planetary missions such as the Europa Orbiter Mission which encountered third-body perturbations from Jupiter causing surface impacts over short time spans [4]. Frozen Low Lunar Orbits (LLO) are of interest to mission designers because their eccentricity and argument of perigee remain fixed over time. Maintaining a constant altitude stable orbit is ideal for lunar reconnaissance missions and requires few orbital maintenance maneuvers. Previously published research has identified four orbital inclinations (e.g., 27°, 50°, 76°, and 86°) , ideal for frozen LLOs, permitting a satellite to remain in a fixed orbit indefinitely [5].

Transferring to/from these stable LLOs from a lunar insertion orbit via single impulse maneuver at the nodal crossing increases the required ΔV proportional to the angular difference. If the Earth's gravitational field were used to change inclination instead of pure thrust, the required ΔV would approach a constant and envelop any inclination change (regardless of angular difference). Traditionally, an orbit transfer is based on underlying two-body dynamics models. For two-body orbit propagation, the trajectory is propagated using Kepler's Equation [6], relating the mean anomaly, M, to the eccentric anomaly, E, and the orbital eccentricity, e, (equal areas are swept out in equal time intervals) such that

$$M = E - e\sin(E). \tag{1}$$

In the presence of large third-body perturbation, the classic assumption underlying the two-body model breaks down due to complex dynamics causing large changes in orbital elements. The underlying assumption that areas of the orbit that are swept out in equal time intervals is not applicable as those areas are no longer equal. Previous research has exploited third-body perturbations to perform plane changes at reduced ΔV when compared to single impulse maneuvers [7] [8] [9]. In practice, the Hughes Global Services 1 Spacecraft (HGS-1) employed this technique to transfer into a low inclination geosynchronous orbit after a launch vehicle stage failure left it in an unusable orbit [10].

Specific to the Earth-Moon three body system, an Earth gravity assisted plane change consists of a tangential impulsive maneuver at a specific location, such that the forces of the other primary (e.g. gravity assist) cause a desired plane

change. The precise location of the first ΔV impulse ensures that a second impulse, performed at next perilune crossing, will lower the apolune inserting the spacecraft into its final orbital configuration. Figure 1 depicts a satellite in a low lunar equatorial orbit making a two-impulse plane change into a polar orbit using an Earth gravity assist.

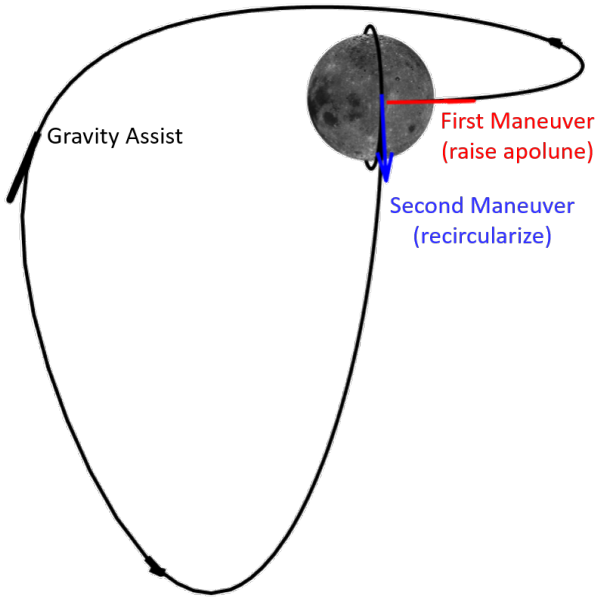

Fig. 1: Properly Scaled Transfer Trajectory of a Two-Impulse Earth Gravity Assisted 90° Inclination Change

Previous research considered plane changes using the Circular Restricted Three-Body Problem (CR3BP). While the CR3BP may be used to estimate the bounds of the required ΔV, ignoring the inclination of the second primary body may leave out entire families of plane changes initiated at lower inclinations. In this work, the transfer trajectory is computed using the full three-body Equations of motion, the latest lunar ephemerides, and solves for the initial conditions via global search optimization methods. Insights from using Earth gravity assists are used to formulate a range of feasible transfer orbit eccentricities centered about the lunar sphere of influence boundary. The analytic approach to solve for the second impulsive ΔV, by assuming a constant Jacobi integral, is extended to include the variation in eccentricity of the transfer orbit.

2. THEORY

2.1 Three-Body Nonlinear Dynamics

Using the same Earth Centered Inertial (ECI) reference frame, the total acceleration from the two primary bodies (Earth and Moon respectively) is provided in Equation 2 [11]

$$\ddot{\vec{r}}_{\oplus sat} = -\mu_{\oplus}\frac{\vec{r}_{\oplus sat}}{r^3_{\oplus sat}} + \mu_{\bigcirc}\left(\frac{\vec{r}_{sat\bigcirc}}{r^3_{sat\bigcirc}} - \frac{\vec{r}_{\oplus\bigcirc}}{r^3_{\oplus\bigcirc}}\right), \tag{2}$$

where $\mu_{\oplus}$ is the standard gravitational parameter of Earth, $\oplus$, and $\mu_{\bigcirc}$ is the standard gravitational parameter of the Moon, $\bigcirc$. The notation $\vec{r}_{\oplus sat}$ represents the position vector of the satellite (sat) with respect to the ECI frame of reference, $\vec{r}_{\oplus\bigcirc}$ represents the location of the moon with respect to Earth (ECI), $\vec{r}_{\bigcirc sat}$ represents the location of the satellite with respect to the moon such that $\vec{r}_{\bigcirc sat} = \vec{r}_{\oplus sat} - \vec{r}_{\oplus\bigcirc}$ and therefore, $\vec{r}_{sat\bigcirc} = -\vec{r}_{\bigcirc sat}$. Note that $\vec{r}_{\oplus\bigcirc}$ and $\dot{\vec{r}}_{\oplus\bigcirc}$ are found from planetary and lunar ephemerides through the CSPICE library routine, `spkezr`, in the J2000 frame of reference [12].

2.1.1 Numerical Simulation of ΔV for a Gravity Assisted Two-Impulse Plane Change

A two-impulse plane change for a spacecraft in a circular LLO is accomplished by determining a transfer trajectory that ensures no burns at apolune. The gravitational pull from the Earth modifies both the energy and angular momentum of the spacecraft (relative to the lunar frame of reference) near apolune. The shape of the transfer trajectory is modified via nonlinear optimization method. The goal of this procedure is to find a return trajectory with a perilune altitude equal to the desired circular lunar orbit and an inclination change equal to a specified amount, Δi.

The first maneuver, parallel to the velocity vector of an equatorial circular orbit about the Moon, consists of fixing the orientation of the transfer orbit relative to Earth. Specifically, the argument of perilune, the eccentricity, and location of Earth relative to the Moon are determined by the transfer epoch, jd_0, via

Initial Circular Orbit		**Transfer Orbit**
a_0	$\rightarrow$	r_p
i_0	$\rightarrow$	i
l_0	$\rightarrow$	ω
ΔV	$\rightarrow$	$a(\Delta V)$
jd_0	$\rightarrow$	jd_0,

The initial state of the transfer trajectory can be computed from parameterizing three variables: the true longitude, $l = \omega + \Omega + \nu$, the initial impulse, ΔV, and the transfer epoch, jd_0. These satisfy:

$$a_{\mathrm{xfer}} = \mu \left[\frac{2\mu}{a_0} - \left(\sqrt{\frac{\mu}{a_0}} + \Delta V \right)^2 \right]^{-1} \tag{3}$$

$$e_{\mathrm{xfer}} = 1 - \frac{a_0}{a_{\mathrm{xfer}}} \tag{4}$$

$$\omega_{\mathrm{xfer}} = l_0 \tag{5}$$

$$i_{\mathrm{xfer}} = \Omega_{\mathrm{xfer}} = \nu_{\mathrm{xfer}} = 0, \tag{6}$$

under the condition that the orbit raising impulse is below the lunar escape velocity, $\Delta V < \left(\sqrt{2}-1\right)\sqrt{\frac{\mu}{a_0}}$. The initial state of the transfer trajectory is converted from Keplerian orbital elements to Moon-centered inertial state vector. The resulting position and velocity of the Moon, corresponding to the initial epoch (jd_0), is added to the Moon-centered state vector to convert to the ECI frame of reference:

$$\begin{aligned} (a_{\mathrm{xfer}}, e_{\mathrm{xfer}}, i_{\mathrm{xfer}}, \omega_{\mathrm{xfer}}, \Omega_{\mathrm{xfer}}, \nu_{\mathrm{xfer}}) &\rightarrow \left(\vec{r}_{\bigcirc sat}, \vec{v}_{\bigcirc sat}\right) \\ \vec{r}_{\oplus sat_0} &= \vec{r}_{\bigcirc sat} + \vec{r}_{\oplus \bigcirc_0} \\ \vec{v}_{\oplus sat_0} &= \vec{v}_{\bigcirc sat} + \vec{v}_{\oplus \bigcirc_0}. \end{aligned}$$

The resulting state vector is propagated forward by numerically integrating the second-order three body Equations of motion (Equation 2). The rate of change of the true anomaly can be found from Kepler's second law of planetary motion:

$$\dot{\nu} = \frac{h}{r^2}, \tag{7}$$

where the magnitude of angular momentum, h, is a function of the current position and velocity of the spacecraft ($h = ||\vec{r} \times \vec{v}||$). The true anomaly is integrated inline with the equations of motion with respect to the second primary. Integration of is terminated when the following two conditions are met: spacecraft trajectory has reached an inflection point between ingressing and egressing from the second primary (see Equations 8-10 for relative change in motion), and $\nu_f > \pi$ ensuring the trajectory is past apolune.

$$u(t) = \begin{cases} \vec{V}_r \cdot \vec{R}_r > 0, & \text{object is egressing} \\ \vec{V}_r \cdot \vec{R}_r = 0, & \text{no relative change} \\ \vec{V}_r \cdot \vec{R}_r < 0, & \text{object is ingressing,} \end{cases} \tag{8}$$

where

$$\vec{V}_r = \vec{v}_{\oplus sat} - \vec{v}_{\oplus\bigcirc} \tag{9}$$

$$\vec{R}_r = \vec{r}_{\oplus sat} - \vec{r}_{\oplus\bigcirc}. \tag{10}$$

Once integration is terminated, the time of flight, t_f, and corresponding state vectors, $\vec{r}_f$, and $\vec{v}_f$, with respect to the second primary are recorded. The pameters ΔV_1, ω_{xfer}, and jd_0 are varied using a particle swarm optimization algorithm [13] until the final position vector magnitude, R_r, and inclination relative to the second primary body, i_f, are within acceptable tolerances of the desired orbit as depicted by:

$$\begin{aligned} \underset{\Delta V_1, \omega_{\text{xfer}}, \text{jd}_0}{\text{minimize}} \quad & \left(\frac{R_r - a_0}{a_0}\right)^2 + \left(\frac{i_f - i_0 - \Delta i}{\pi}\right)^2 \\ \text{subject to} \quad & 0 < \Delta V_1 < (\sqrt{2}-1)\sqrt{\frac{\mu}{a_0}}, \\ & 0 \leqslant \omega_{\text{xfer}} < 2\pi, \\ & \text{jd}_{\text{min}} \leqslant \text{jd}_0 \leqslant \text{jd}_{\text{max}}, \\ & u(t_f) = 0, \\ & \pi \leqslant \nu_f \leqslant 2\pi. \end{aligned} \tag{11}$$

The initial epoch is allowed to vary a full lunar month, $\text{jd}_{\text{max}} = \text{jd}_{\text{min}} + 28$, to capture all possible lunar inclinations and relative angles to the transfer trajectory. After running nonlinear optimization, the second impulse, ΔV_2 is found from circularizing the transfer orbit at t_f, such that $\Delta V_2 = \sqrt{\frac{\mu}{r_f}} - v_f$. The total required $\Delta V_{2\text{-burn}}$ is then the sum of the two:

$$\Delta V_{2\text{-burn}} = \Delta V_1 + \Delta V_2. \tag{12}$$

Note for cases where the final orbit apolune is greater than perilune, $r_a > r_f$, the second impulse can be computed by

$$\Delta V_2 = \sqrt{\frac{2\mu}{r_f} - \frac{2\mu}{r_a + r_f}} - v_f. \tag{13}$$

2.1.2 Analytic Bounds of ΔV for a Gravity Assisted Two-Impulse Plane Change

Hill's problem, a variant of the classic restricted three-body problem, was first proposed by Hill for studying the motion of the Moon. In this case, the massless body is attracted by two primary bodies of unequal mass $m_2 << m_1$. In a rotating coordinate system, the smaller primary is located at the origin while the positive x-axis is parallel to the two primaries. Hill's Equations are expressed as [14]:

$$\ddot{x} = -\frac{x}{r^3} + 3x + 2\dot{y}, \;\; \ddot{y} = -\frac{y}{r^3} - 2\dot{x}, \;\; \ddot{z} = -\frac{z}{r^3} - z, \tag{14}$$

where $r = \sqrt{x^2 + y^2 + z^2}$ is the distance of the satellite from the secondary body. The unit length and time scales are $l = (\mu/N^2)^{1/3}$ and $\tau = 1/N$ respectively (N is the angular velocity of the frame and μ is the gravitational parameter of the attracting body). Equation 14 has only one known integral identified as the Jacobi Integral, a combination of the spacecraft energy and angular momentum,

$$J = \frac{1}{2}v^2 - \frac{1}{r} - \frac{1}{2}\left(3x^2 - z^2\right) = \frac{1}{2}v^2 - \frac{1}{r} - h\cos(i) + \frac{1}{2}r^2 - \frac{3}{2}x^2, \tag{15}$$

where r, v, h, and i represent the magnitude of the position, velocity, angular momentum, and inclination vectors in inertial space, with the same origin as the rotating frame with respect to the second primary. One unique property of the Jacobi Integral is that it remains constant in the rotating frame (see Equation 16) as the total energy cannot change. The difference in altitude between the initial transfer orbit segment and final transfer orbit segment is assumed to be zero ($\Delta r_p = 0$).

$$\Delta J = J_f - J_0 = \frac{1}{2}(v_f^2 - v_0^2) - r_p v_f \cos(i_0 + \Delta i) + r_p v_0 \cos(i_0) - \frac{3}{2}(x_f^2 - x_0^2) = 0, \tag{16}$$

where the magnitude of the angular momentum vector is expressed as $h = r_p v$. The final velocity, v_f, can be found by re-arranging Equation 16 and using the solution of the reduced quadratic equation:

$$v_f = r_p \cos(i_0 + \Delta i) \pm \sqrt{r_p^2 \cos^2(i_0 + \Delta i) + v_0^2 - 2 r_p v_0 \cos(i_0) + 2c}, \tag{17}$$

where $c = \frac{3}{2}\left(x_f^2 - x_0^2\right)$. The initial dimensionless orbital velocity can be expressed in terms of the transfer trajectory r_p and r_a at periapsis as $v_0 = \frac{1}{r_p}\sqrt{\frac{2r_a}{r_p + r_a}}$, c depends on ω and Ω and is bounded by $-\frac{3}{2} r_p^2 \cos^2(i_0) \leqslant c \leqslant \frac{3}{2} r_p^2 \cos^2(i_0 + \Delta i)$ [7]. Substituting this inequality into Equation 17, the final velocity of the transfer orbit at periapsis is bounded by,

$$v_f^- \leqslant v_f \leqslant v_f^+. \tag{18}$$

The $\pm$ sign is dropped as subtracting the two velocity components provides an identical velocity magnitude with an opposite sign. $v_0^{\pm}$ is substitued for v_0 to account for variation in the eccentricity of the transfer orbit (see Equations 25-26). Note that the distance and velocity in Equations 19-20 are normalized so the resulting velocities must be rescaled by l/τ:

$$v_f^- = r_p \cos(i_0 + \Delta i) + \sqrt{r_p^2 \cos^2(i_0 + \Delta i) + \left(v_0^-\right)^2 - 2 r_p v_0^- \cos(i_0) - 3 r_p^2 \cos^2(i_0)} \tag{19}$$

$$v_f^+ = r_p \cos(i_0 + \Delta i) + \sqrt{4 r_p^2 \cos^2(i_0 + \Delta i) + \left(v_0^+\right)^2 - 2 r_p v_0^+ \cos(i_0)}. \tag{20}$$

The second impulse, ΔV_2, is a function of the circular velocity subtracted from the final velocity such that $\Delta V_2 = \sqrt{\frac{\mu}{r_p}} - v_f$. The first impulse, ΔV_1, is a function of the transfer orbit apogee, which can vary in altitude around the sphere of influence (SOI),

$$r_{SOI} \approx a \left(\frac{\mu_2}{\mu_1}\right)^{2/5}, \tag{21}$$

where μ_2/μ_1 is the mass ratio of the two primaries, and a is the average distance between the two primaries. The eccentricity of the transfer orbit that approaches the SOI is then

$$e_{\mathrm{SOI}_{xfer}} = 1 - \frac{2 r_p}{r_p + r_{SOI}}. \tag{22}$$

The apoapsis of the transfer orbit may vary about the sphere of influence of the second primary ($e_{\mathrm{xfer}} = e_{\mathrm{SOI}_{xfer}} \pm \Delta e$) serving as a bounding case for its semi-major axis:

$$\frac{r_p}{1 - e_{\mathrm{SOI}_{xfer}} + \Delta e} \leqslant a_{\mathrm{xfer}} \leqslant \frac{r_p}{1 - e_{\mathrm{SOI}_{xfer}} - \Delta e}. \tag{23}$$

The transfer orbit velocity at periapsis is found from $v_0 = \sqrt{\frac{2\mu}{r_p} - \frac{\mu}{a_{\mathrm{xfer}}}}$ and bounded by:

$$v_0^- \leqslant v_0 \leqslant v_0^+. \tag{24}$$

Here,

$$v_0^- = \sqrt{\frac{\mu}{r_p}\left(1 + e_{\mathrm{SOI}_{xfer}} - \Delta e\right)} \tag{25}$$

$$v_0^+ = \sqrt{\frac{\mu}{r_p}\left(1 + e_{\mathrm{SOI}_{xfer}} + \Delta e\right)}. \tag{26}$$

The required first impulse to transfer from a circular orbit to the transfer orbit is then $\Delta V_1 = v_0 - \sqrt{\frac{\mu}{r_p}}$. The total $\Delta V = |\Delta V_1| + |\Delta V_2|$ for the two-burn transfer is then bounded:

$$v_0^- + v_f^m - 2\sqrt{\frac{\mu}{r_p}} \leqslant \Delta V_{2-\mathrm{burn}} \leqslant v_0^+ + v_f^+ - 2\sqrt{\frac{\mu}{r_p}}. \tag{27}$$

2.2 Two-Body Nonlinear Dynamics

Equation 2 can be reduced to the well known two-body Equations of motion assuming that the second primary body mass is infinitesimally small, $\mu_{\bigcirc} = 0$:

$$\ddot{\vec{r}} = -\mu \frac{\vec{r}}{r^3}. \tag{28}$$

Where μ is the standard gravitational parameter of the primary closest to the satellite (primary body), and $\vec{r}$ is the three-dimensional inertial position vector with respect to the primary body.

2.2.1 Analytic ΔV for a Single Impulse Plane Change

Assuming a circular orbit around the primary body, the analytical solution for a pure inclination change in a two-body environment is computed by a single impulse at the nodal crossing [11]:

$$\Delta V_{\text{1-burn}} = 2\sqrt{\frac{\mu}{a}} \sin\left(\frac{\Delta i}{2}\right), \tag{29}$$

where a is the semi-major axis of the circular orbit, and Δi is the change in inclination needed.

2.2.2 Analytic ΔV for a Three Impulse Plane Change

Depending on the amount of inclination change needed, a bi-elliptic plane change is commonly used. A bi-elliptic plane change consists of three impulses (ΔV_1, ΔV_2, and ΔV_3). The first maneuver is a coplanar orbit raise such that the semi-major axis of the transfer orbit, a_{xfer}, is found from Equation 3. The largest initial coplanar impulse allowable for a bi-elliptic transfer is governed by the escape velocity of the primary such that [15]:

$$\Delta V_1 < \left(\sqrt{2} - 1\right)\sqrt{\frac{\mu}{a}}. \tag{30}$$

The radius of apogee for the coplanar transfer orbit is then found from:

$$r_{a_{\text{xfer}}} = 2a_{\text{xfer}} - a. \tag{31}$$

The ΔV required for a plane change at the apogee of the transfer orbit is considered the second impulse,

$$\Delta V_2 = \sqrt{2} V_{\text{xfer}} \sqrt{(1 - \cos\Delta i)}, \tag{32}$$

where

$$V_{\text{xfer}} = \sqrt{\frac{2\mu}{r_{a_{\text{xfer}}}} - \frac{\mu}{a_{\text{xfer}}}}. \tag{33}$$

The third impulsive maneuver is made at the perigee of the transfer orbit to circularize the trajectory at the original semi-major axis, a, such that:

$$\Delta V_3 = \sqrt{\frac{2\mu}{a} - \frac{\mu}{a_{\text{xfer}}}} - \sqrt{\frac{\mu}{a}}. \tag{34}$$

The total ΔV required for a three-impulsive maneuver transfer is then the sum of all three burns. The bi-elliptic transfer then becomes a minimization problem:

$$\begin{aligned} &\text{minimize} \quad \Delta V_{\text{3-burn}} = \sum_{i=1}^{3} \Delta V_i \\ &\text{subject to} \quad 0 \leqslant \Delta V_1 < \left(\sqrt{2} - 1\right)\sqrt{\frac{\mu}{a}}. \end{aligned} \tag{35}$$

Notice that when $\Delta i << 90^\circ$, minimizing Equation 35 will converge to Equation 29 as $\Delta V_{\text{3-burn}} \rightarrow \Delta V_1$.

3. SIMULATION AND VERIFICATION

Using the methodology outlined in section 2.1.1, circular equatorial LLOs were created with surface altitudes ranging from 100 km to 1,200 km (circular orbit altitudes above 1,200 km are unstable [3]). The position of the moon with respect to the ECI J2000 coordinate system was found from the DE440 short planetary ephemeris [16] between the dates of 01/01/2030 and 01/29/2030. The SOI radius was computed using the closest approach distance between the two primaries, 362974.52 km, via Equation 21.

The analytic bounds for the Earth gravity assisted two-impulse plane change were computed from Equation 27. The eccentricity of the transfer orbit varied about the SOI boundary (Equation 22) such that $e_{\mathrm{SOI}_{xfer}} + [-0.10, +0.06]$. Results of the numerical simulation, using particle swarm optimization, are displayed in Table 1. Note that the transfer trajectory argument of perilune, time of flight, and total ΔV are included for circular orbit altitudes between 100 to 1,200 km.

Perilune Alt	**Eccentricity**	**Arg of Perilune**	**Time of Flight**	**Total ΔV**	**ΔV Analytic Bounds**
100 km	0.90 - 0.95	19.14 - 317.50°	2.41 - 7.80 Days	1.23 - 1.30 km/s	1.16 - 1.35 km/s
200 km	0.85 - 0.95	15.30 - 346.27°	1.51 - 6.83 Days	1.15 - 1.27 km/s	1.12 - 1.31 km/s
500 km	0.84 - 0.94	45.55 - 349.06°	1.74 - 8.31 Days	1.06 - 1.16 km/s	1.03 - 1.20 km/s
750 km	0.85 - 0.93	14.02 - 359.11°	2.39 - 7.35 Days	1.01 - 1.09 km/s	0.97 - 1.13 km/s
1,000 km	0.83 - 0.93	6.44 - 322.91°	2.23 - 9.21 Days	0.94 - 1.07 km/s	0.92 - 1.07 km/s
1,200 km	0.82 - 0.92	49.77 - 348.74°	2.48 - 8.05 Days	0.91 - 1.00 km/s	0.88 - 1.03 km/s

Table 1: Perilune Altitude, Eccentricity, Argument of Perilune, Time of Flight, and Total ΔV of Transfer Trajectories for Earth Gravity Assisted Inclination Changes Between Circular Orbits

Figure 2 compares the numerical results of a two-impulse transfer, $\Delta V_{2\mathrm{B}}$, under the full three-body Equations of motion to the analytic bounds, $\Delta V_{2\mathrm{B\text{-}bounds}}$, as computed in Table 1. It also shows the results of using a single-impulse, $\Delta V_{1\mathrm{B}}$, (plane change occurs at the ascending node), and an optimal three-impulse plane change, $\Delta V_{3\mathrm{B}}$. The later using the bi-elliptic plane change technique overviewed in section 2.2.2, under the simplified two-body equations of motion.

Numerical results are bounded by the analytic technique. Raising the apolune into the SOI boundary with a two-impulse maneuver strategy provides a ΔV savings for inclination changes greater than 45 degrees ($\Delta i > 45°$). The ΔV required for the two-impulse maneuver is less than the theoretical minimum ΔV using a bi-elliptic transfer nearing escape velocity. Figure 3 depicts the cost savings of using an Earth gravity assist plane change strategy, over that of a single-impulse plane change, across a variety of circular orbit altitudes and inclination changes. Small cost savings in ΔV start near inclination changes of 45°, and increase up to 60% savings for plane changes greater than 135°. Note that the Δi required to achieve the same cost savings decreases as altitude is increased.

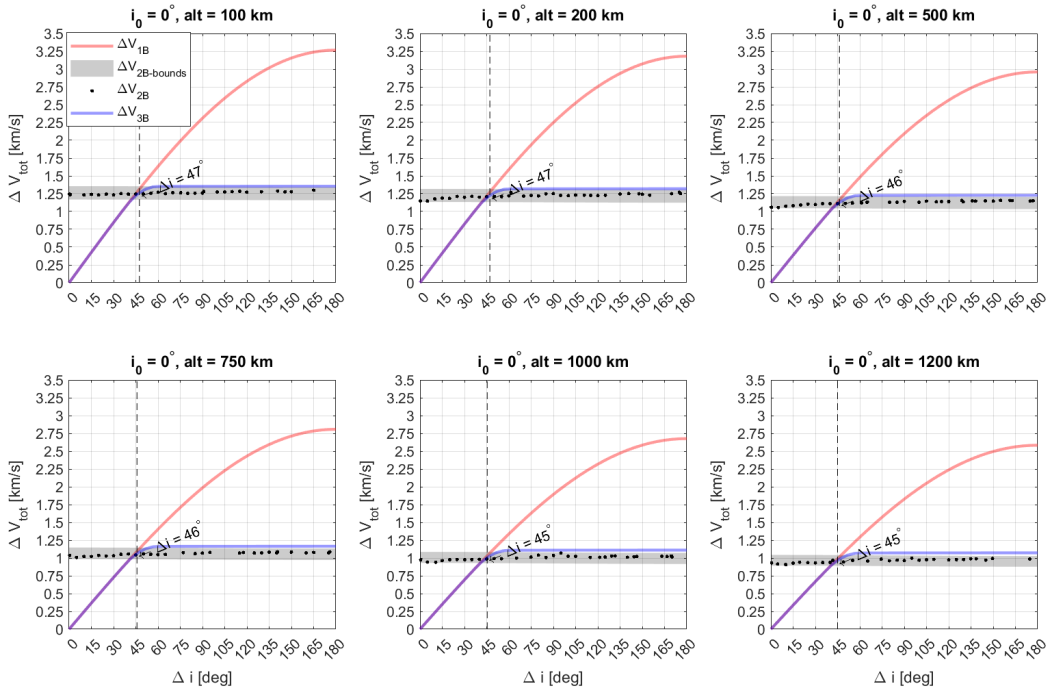

Fig. 2: ΔV Comparison of 1-3 Impulse Plane Change Techniques. 1-burn and 3-burn assume underlying two-body dynamics while the 2-burn maneuver is found from an Earth gravity assisted plane change using three-body dynamics. The 2B-Bounds are analytic bounds of Gravity assisted two-impulse plane changes. 2B represents numerically optimized results.

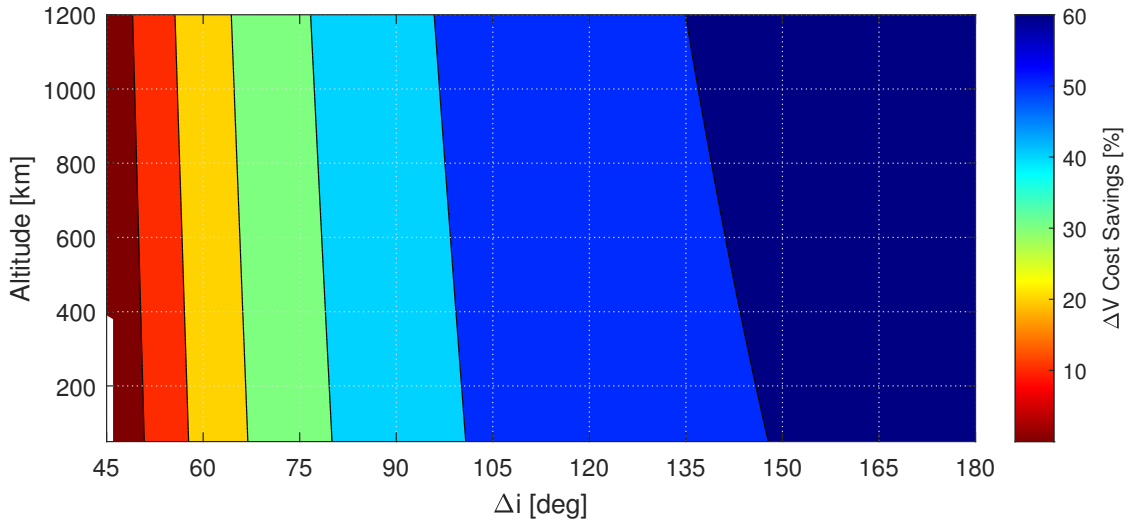

Fig. 3: ΔV Savings of Using a Two-Impulse Earth Gravity Assist over a Single Impulse Instantaneous Plane Change

4. CONCLUSIONS AND FUTURE WORK

Inclination change maneuvers for lunar orbits perturbed by the Earth's gravity have been analyzed numerically, and verified with circular restricted three-body analytic theory. The restricted three-body analytic theory was extended to include a variation of eccentricity about the lunar sphere of influence. Earth gravity assisted inclination changes require less ΔV above inclination changes of 45°, when compared to single-impulse and near infinite apolune bi-elliptic plane change strategies. For lunar orbital altitudes greater than 100 km, the total ΔV required for an Earth gravity assisted inclination change is less than 1.4 km/s (regardless of the plane change angle) with a transfer duration of less than ten days. Exploiting Earth's gravity to change the inclination of a lunar orbit allows for a spacecraft to reduce fuel costs up to 60%. Since the orbit of the Moon is slightly inclined, inclination changes covering the entire range of starting inclinations ($(\Delta i, i_0) \in [0, 180°]$) are feasible at some Moon-Earth geometry occurring over a lunar month.

For future work, multi-revolution gravity assist trajectories can be found from stopping numerical integration of Equation 7 after some integer multiple, N_{rev}, of π such that $\nu_f > N_{rev}\pi$ where $N_{rev} > 1$. This reduces the ΔV costs associated with specific plane change maneuvers even further. The right ascension of the ascending node changes as a function of the Earth-Moon geometry, lunar oblateness, orbital eccentricity and semi-major axis. Similar low Earth constellation configuration techniques may be used to simultaneously control inclination and right ascension of the ascending node.

5. ACKNOWLEDGMENTS

The authors would like to thank J.R Jordan, Jeremy Kalina, and Mark Gould of Raytheon Intelligence & Space for their support, encouragement, and funding of this research.

6. REFERENCES

[1] T. Bell, "Bizar lunar orbits," *NASA Science News, November*, vol. 30, 2006.
[2] M. Lidov, "Evolution of the orbits of artificial satellites of planets as affected by gravitational perturbation from external bodies," *AIAA Journal*, vol. 1, no. 8, pp. 1985–2002, 1963.
[3] T. Bell, "A new paradigm for lunar orbits," *NASA Science News, November*, vol. 30, 2006.
[4] B. Villac and D. Scheeres, "New class of optimal plane change maneuvers," *Journal of guidance, control, and dynamics*, vol. 26, no. 5, pp. 750–757, 2003.
[5] J. F. San-Juan, R. López, and I. Pérez, "High-fidelity semianalytical theory for a low lunar orbit," *Journal of Guidance, Control, and Dynamics*, vol. 42, no. 1, pp. 163–167, 2019.
[6] J. R. Voelkel, *The composition of Kepler's Astronomia nova*. Princeton University Press, 2001.
[7] B. F. Villac and D. J. Scheeres, "Optimal plane changes using third-body forces," *Annals of the New York Academy of Sciences*, vol. 1017, no. 1, pp. 255–266, 2004.
[8] B. F. Villac and D. J. Scheeres, "Third-body-driven vs. one-impulse plane changes," *The Journal of the Astronautical Sciences*, vol. 57, no. 3, pp. 545–559, 2009.
[9] R. Aravind, S. Harsh, and P. Bandyopadhyay, "Mission to retrograde geo-equatorial orbit (rgeo) using lunar swing-by," in *2012 IEEE Aerospace Conference*, pp. 1–8, IEEE, 2012.
[10] C. Ocampo, "Trajectory analysis for the lunar flyby rescue of asiasat-3/hgs-1," *Annals of the New York Academy of Sciences*, vol. 1065, no. 1, pp. 232–253, 2005.
[11] D. A. Vallado, *Fundamentals of astrodynamics and applications*, vol. 12. Springer Science & Business Media, 2001.
[12] J. L. Hilton, C. Acton, J.-E. Arlot, S. A. Bell, N. Capitaine, A. Fienga, W. M. Folkner, M. Gastineau, D. Pavlov, E. V. Pitjeva, *et al.*, "Report of the iau commission 4 working group on standardizing access to ephemerides and file format specification," *arXiv preprint arXiv:1507.04291*, 2015.
[13] J. Kennedy and R. Eberhart, "Particle swarm optimization," in *Proceedings of ICNN'95-international conference on neural networks*, vol. 4, pp. 1942–1948, IEEE, 1995.
[14] V. Szebehely, "Theory of orbits," 1967.
[15] P. Khatri, M. Gautam, and A. PR, "Principles of physics," *Kathmandu: Ayam Publication*, p. 170, 2010.
[16] R. S. Park, W. M. Folkner, J. G. Williams, and D. H. Boggs, "The jpl planetary and lunar ephemerides de440 and de441," *The Astronomical Journal*, vol. 161, no. 3, p. 105, 2021.